Proceedings of Meetings on Acoustics

166th Meeting of the Acoustical Society of America
San Francisco, California
2 - 6 December 2013

Session 4aNS: Noise

4aNS6. Intensity analysis of the dominant frequencies of military jet aircraft noise

Trevor A. Stout*, Kent L. Gee, Tracianne B. Neilsen, Alan T. Wall and Michael M. James

*Corresponding author's address: Department of Physics and Astronomy, Brigham Young University, Provo, Utah 84602, tstout@byu.edu

  Acoustic intensity measurements of the F-22A Raptor are analyzed as part of ongoing efforts to characterize the noise radiation from military jet aircraft. Data were recorded from an array of microphones and an attached tetrahedral intensity probe at various locations to the sideline and aft of the aircraft. Recently, techniques such as coherence, similarity spectra analyses, and near-field acoustical holography have indicated a peak-frequency region comprised of two maxima (not accounted for by current jet noise models) that have very different radiation directionalities. Acoustic vector intensity is analyzed as a function of frequency to further assess the behavior of this double-peak phenomenon. In addition, a simulation using an equivalent source model with two mutually incoherent, directional line arrays yields numerical intensity results that exhibit the same trends as the measured intensity. The results provide further evidence that high-performance military jet noise contains a double spectral peak in the maximum radiation direction that is not present in laboratory-scale jets. [Work supported by ONR].

INTRODUCTION

Acoustic intensity measurements of the F-22A Raptor have been analyzed as part of ongoing efforts to characterize the noise radiating from military jet aircraft. In addition, array-based methods using measurements outside of the jet plume have been used to study important acoustic quantities. Techniques such as beamforming,[1] near-field acoustical holography,[2,3,4] coherence analysis methods, etc. have previously been applied to predict the frequency-dependent nature of sound radiation and source location within the plume.

Intensity, a direct measure of energy flow in a sound field, has not seen much application to jet noise analysis. However, measurement of the vector intensity can provide a map of the frequency-specific sound radiation from turbulent flows. For example, Jaeger and Allen[5] used a two-dimensional intensity probe to characterize source location within jet plumes of Mach numbers 0.2-0.6, one of the most in-depth applications to aeroacoustics. Recently, three-dimensional intensity probes have been used to measure the sound field of a solid rocket motor plume.[6,7,8] The same probe design was also used to make near-field acoustic intensity measurements of the F-22A Raptor. The intensity probe was attached to the top of a 90-microphone rectangular array of microphones, which was moved to multiple locations to the sideline and aft of the aircraft.
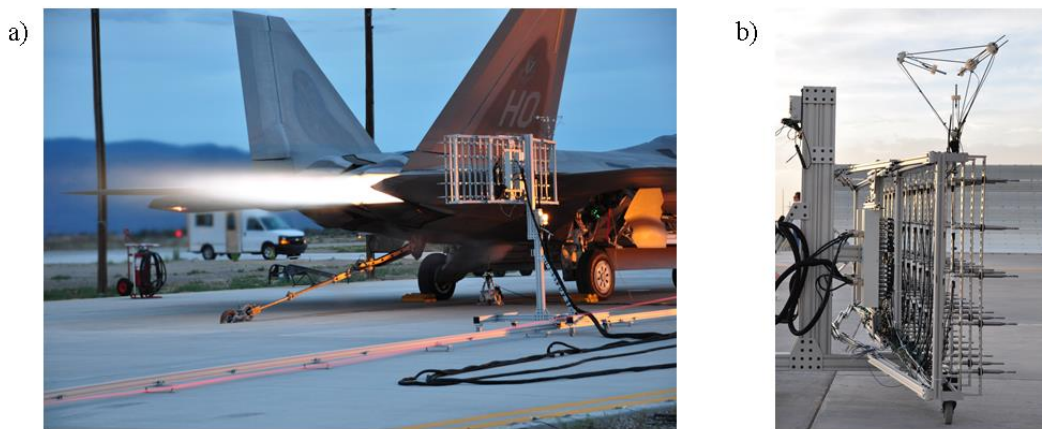

FIGURE 1. (a) F-22 engine firing with rig and probe in place, and (b) close-up of the intensity probe positioned on top of the microphone array. The array and probe took measurements at several locations along guide rails while the engine was cycled through four power conditions.

Figure 2 describes the physical layout of the measurements. The F-22 was tethered to the center of a concrete run-up pad, and one engine was run up to different conditions while the other was held at idle. The rectangular array and intensity probe were used to acquire measurements at each location for four different conditions: idle, intermediate (80% throttle), military (full throttle), and afterburner. Multiple references explain the procedure and measurement apparatus.[9,10] In this paper, the intensity measurements are used to explore some unexpected results found by other analysis methods in the peak-frequency region of the F-22 spectrum.
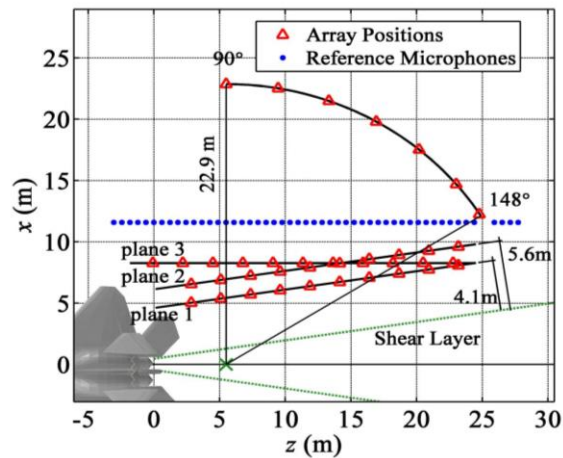
FIGURE 2. Top-down schematic of data locations for the F-22 measurements. The red triangles indicate the center of the microphone rig with the intensity probe attached. The mark at 5.5 m downstream describes the estimated source location, set as the center of the 22.9m arc. The blue dots show locations for the ground-based reference array.

SPECTRAL ANALYSIS

Using data from the array microphones and ground-based reference microphones, multiple analysis techniques have been used to examine the peak-frequency region (from about 100-325 Hz) of the F-22 spectrum. The spectrum recorded at the ground-based microphone locations was matched to two similarity spectra curves, which correspond to radiation from large and fine-scale turbulence structures.[11,12] Currently, this generalized two-source representation is a prevalent model used in jet plume source characterization. Except at high frequencies, the similarity spectra curves follow the measured data well in the general frequency trend (from low frequency to several kHz).

The similarity curves, however, do not account for a double peak in the measured spectra. Recently, discrete frequency peaks were discovered,[4,11] from what appear to be two mutually-incoherent sources which exhibit distinct directionalities.[13] As seen in Fig. 3, the spectrum shifts from a maximum at about 250 Hz at 120° to 125 Hz at 140°, without a smooth transition between these frequencies. The discrete nature of the spectral maxima in the peak-frequency region when considering the different radiation directions suggest a shortcoming in the similarity spectra model in the peak-frequency region.
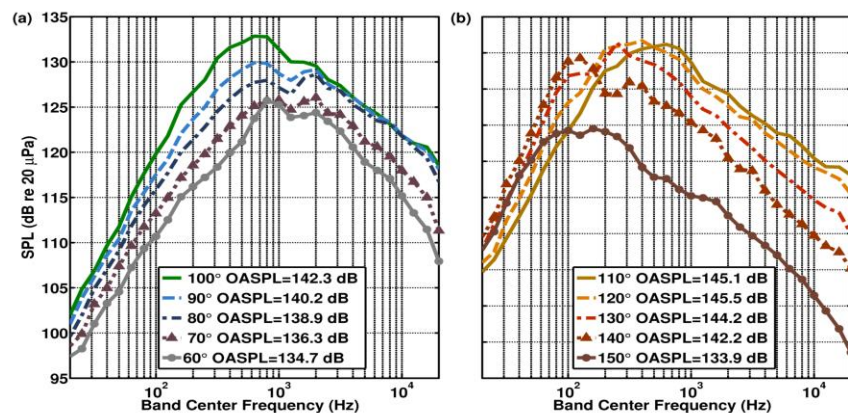

FIGURE 3. One-third octave sound pressure levels measured according to direction from assumed source (5.5 m downstream), for military engine conditions (compare the same for afterburner in Ref. 11).

Another way to visualize the spatial variation in frequency content is to examine spectral maps across the ground array. An example of such a map at military power is displayed in Fig. 4 and shows two distinct lobes – regions of high levels – centered at about 125 Hz and 400 Hz. Between about 8 m and 24 m downstream, these lobes dominate the radiation. In the middle region, between ~14-18 m, a single microphone receives the superposition of both spectral lobes, which causes a dual peak in the spectrum. Looking from upstream to downstream in this region, the spectral maximum shifts from one lobe to the other, as seen in Fig. 3.
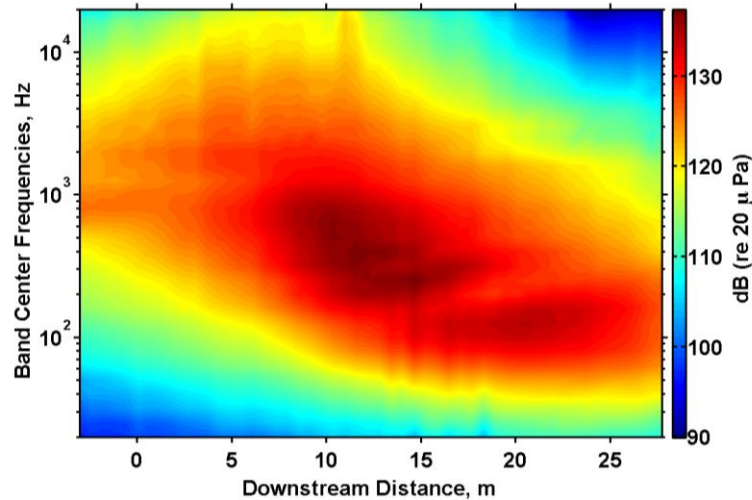
FIGURE 4. One-third-octave SPL recorded by the ground microphone array for military engine conditions. Note the two distinct high-level regions centered about 125 Hz and 400 Hz that dominate the radiation from 8m to 24 m downstream.

Not only the ground microphone array, but data from the 90-microphone array also exhibits the dual spectral lobes. Figures 7(a) and 8(a) show the one-third-octave SPL recorded by the rig for military and afterburner engine conditions along the measurement plane 4.1 m from the shear layer (plane 1). Again, the dual spectral lobes are apparent as the spectral maximum jumps from 250 Hz to 125 Hz at 10.5-11 m downstream.

To investigate the nature of the two radiation lobes, the coherence between microphones in the ground-based array was analyzed in the peak-frequency region. Fig. 5 shows the results at 200 Hz. The spatial coherence has two lobes of high coherence (at Z = 9-16 m and past Z = 20 m) that correspond to the locations of highest recorded sound power at that frequency (see bottom SPL plot). The fact that there is low coherence between microphones in these two spatial regions, and in between them as well, indicates that the mechanisms responsible for the radiation at those locations are not coherent with each other. This is supported by previous near-field acoustical holography (NAH) results, which reconstructed orthogonal partial fields with distinct directionalities.[14] Because of the way the partial fields were chosen, this result also suggests two independent source mechanisms that have different directionalities and which radiate with discrete spectral maxima. The hypothesis is tested below in a series of intensity simulations.
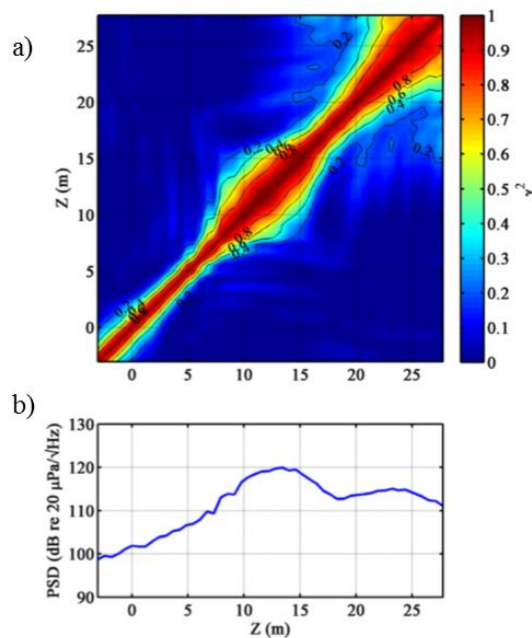

FIGURE 5. (a) Coherence between microphones along the ground-based array at 200 Hz. (b) Power spectral density (PSD) values at 200 Hz, along ground-based array. Note the two lobes of high coherence at Z = 9-16 m and past Z = 20 m.

INTENSITY MEASUREMENTS

Acoustic intensity vectors were calculated in the usual way based on finite-difference techniques with cross-spectra from the four intensity probe microphones.[16] According to the tetrahedral probe geometry, the various cross-spectral components were weighted and summed to give intensity components along the three cardinal directions using the least-squares technique developed by Pascal and Li.[17] The resulting single-frequency intensity vectors are plotted, as in Fig. 6, at the measurement locations along plane 2 (see Fig. 2) to give an indication of the flow of the sound near the F-22. For each frequency, a 3 dB-down region from the maximum intensity vector was identified. Intensity vectors from the 3 dB-down region were traced back to the jet center line as a method of approximating source location.
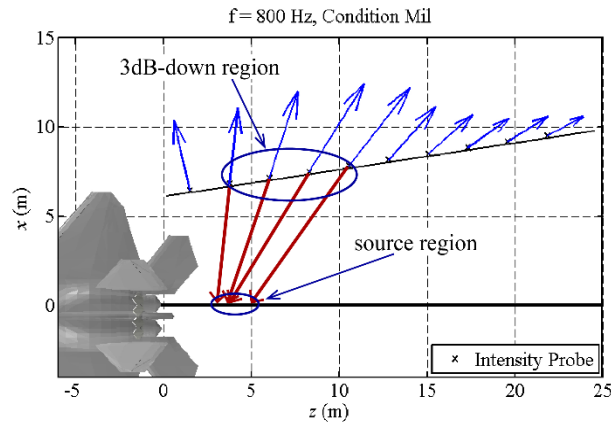

FIGURE 6. Intensity results (blue arrows) at 800 Hz, including an example 3 dB-down region, shown as a circle on the second measurement plane. The intensity vectors are traced backwards to the jet centerline (red lines) to give an estimated source region at this frequency.

The approximate source regions obtained from the intensity vectors from measurement plane 2 confirm the general frequency trend expected of radiation from jet plumes. The generalized source region contracts and moves upstream with increasing frequency, as predicted by beamforming results from multiple studies.[1,18] Figures 7(b) and 8(b) show the approximate source location regions for military and afterburner conditions, respectively. These approximate source regions show the same general trends as the spatial variation in the spectral maxima measured along plane 1 using the rectangular 90-microphone array (Figs. 7(a), 8(a)). While results from the two engine conditions are similar, the source region above 200 Hz at afterburner remains broader and extends farther downstream than for military.
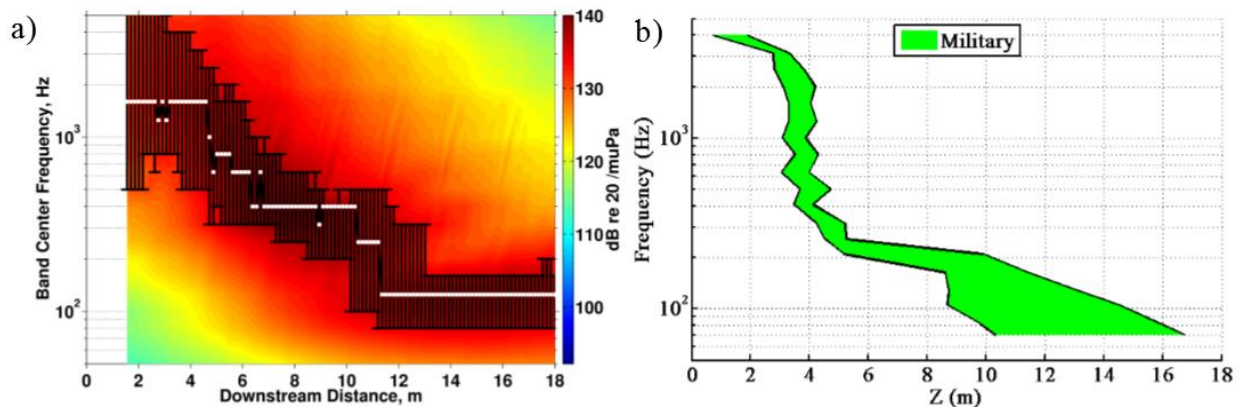

FIGURE 7. (a) Height-averaged one-third-octave spectra as measured on the 90-microphone rig at 4.1 m from the shear layer (plane 1), and (b) generalized source location region vs frequency based on intensity results for military engine conditions. Error bars in (a) indicate

regions within 3 dB of the spectral maximum, which is indicated as a white dot. At about 11 m downstream, the peak frequency jumps from 250 to 125 Hz. Left and right bounds in (b) describe the edges of the generalized source region estimated from tracing the intensity vectors within 3dB of the maximum; note how the source contracts and moves upstream rapidly after 200 Hz.
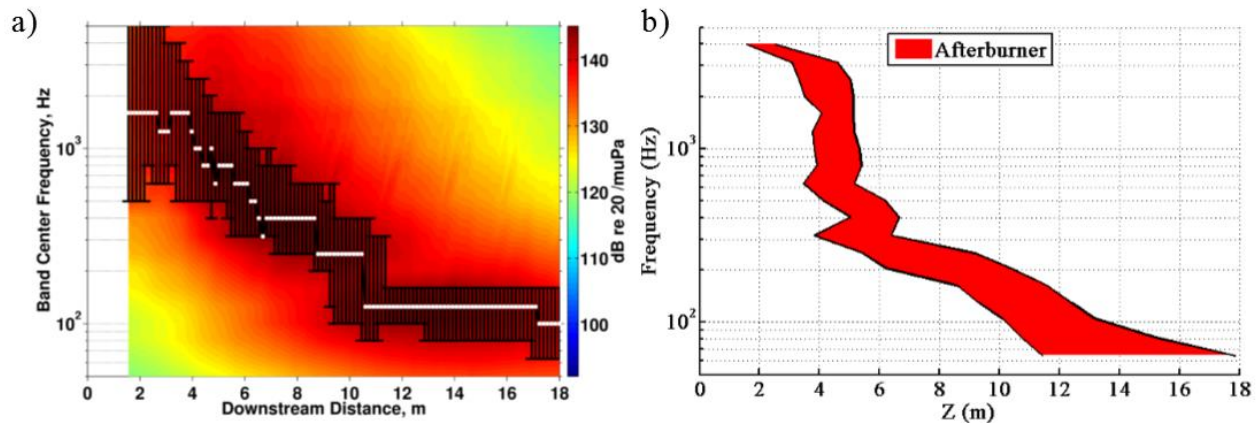

FIGURE 8. (a) Height-averaged one-third-octave spectra as measured on the 90-microphone rig at 4.1 m from the shear layer (plane 1) and(b) generalized source location region vs frequency based on intensity results for afterburner engine conditions. As in Fig. 7, error bars in (a) indicate regions within 3 dB of the spectral maximum, which is indicated as a white dot. At about 10.5 m downstream, the peak frequency jumps from 250 to 125 Hz. Left and right bounds in (b) describe the edges of the generalized source region; note how the source contracts and moves upstream rapidly after about 200 Hz. However, the source region remains broader and extends farther downstream than in Fig. 7(b).

Figs. 9-11 show intensity measurements in the peak-frequency region. Between results from 136 Hz to 316 Hz, the maximum intensity region shifts from about Z = 20 m farther upstream to about Z = 10 m. Figs. 9 and 11 show radiation with intensity maxima centered on about Z = 20 and Z =10 m, respectively. In Fig. 10, the radiation at 232 Hz produces two spatially distinct intensity maxima. The presence of these maxima can be predicted by close scrutiny of the dual spectral lobes in Fig. 4. At 232 Hz both lobes are present with distinct spatial locations, while at 136 Hz or 316 Hz only one spectral lobe contributes primarily.

These intensity measurements point to the possibility of two distinct source mechanisms predominantly responsible for radiation in the peak-frequency region. Supposing the presence of these two sources, Figs. 9-11 can be interpreted in terms of the source contributions to overall radiation. Between 125 and 315 Hz, the dominating radiation shifts from one source to the other. At 136 Hz, radiation is dominated by one source which radiates at about 140 degrees (relative to the engine inlet). At 232 Hz, contributions from both sources can be seen. At 316 Hz, the second source dominates, radiating at about 120 degrees.
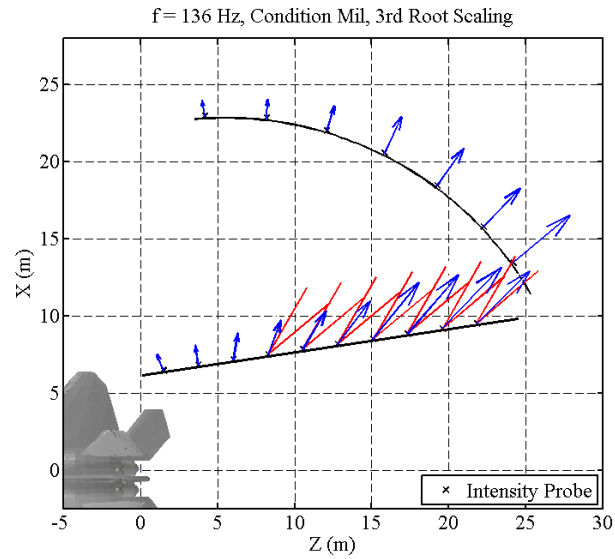
FIGURE 9. Intensity measurements (blue arrows) at 136 Hz, military condition on plane 2 and the arc at 23 m. The red lines indicate 120 and 140 degrees relative to the engine inlet. The radiation at this frequency is dominated by one intensity maximum at Z = 20 m.
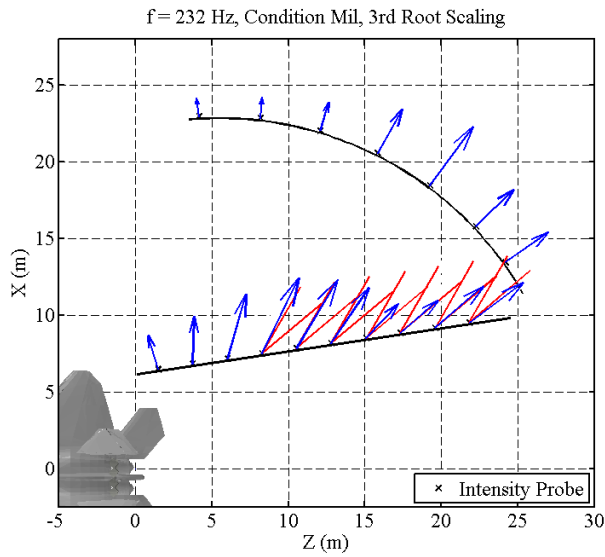

FIGURE 10. Similar to Fig. 9. Intensity measurements at 232 Hz, military condition. Note how the radiation at this frequency produces two distinct maxima, seen spatially at about Z = 10 m and Z= 20 m.
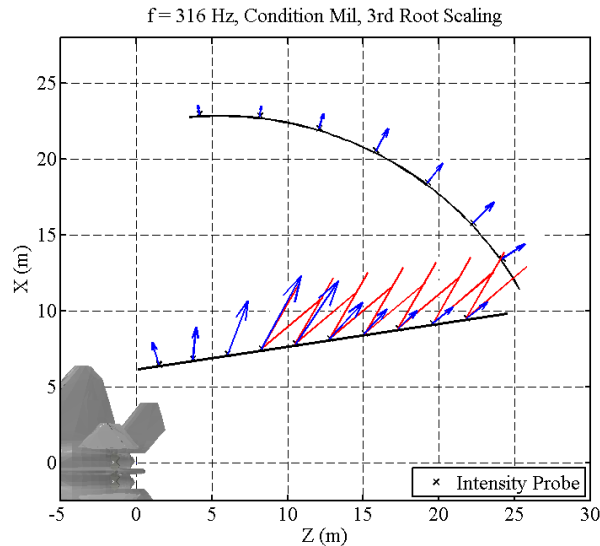
FIGURE 11. Similar to Fig. 9. Intensity measurements at 316 Hz, military condition. The radiation at this frequency is dominated by one intensity maximum at $Z = 10$ m.

INTENSITY SIMULATIONS

To test the hypothesis that the dual lobe could be created by two independently radiating (i.e., incoherent) sources, an equivalent source model involving two line arrays of closely-spaced monopoles has been created. The model is similar to one previously used, which was designed to match to SPL at the rig locations.[15] In this previous method, large and fine-scale radiation was modeled using two line arrays at the same locations along the jet axis, one correlated (thus, directional) and the other uncorrelated. In contrast, the current model seeks to simulate the frequency-dependent intensity patterns using two, self-coherent, mutually incoherent equivalent sources (without attempting to make connections to fine-scale or large-scale flow properties). In addition, the current model is designed to be operational over a range of frequencies, rather than requiring the development of a new model for each frequency. The predictions are matched to intensity measurements rather than SPL.

The features of the two sources, suggested by the aforementioned analysis techniques and intensity measurements, include variation in source locations, radiation directions, and spectra. Monopoles are placed 2 cm apart, starting at $Z = 0$ m (the engine nozzle) and ending at $Z = 20$ m. Gaussian noise from each monopole is time-delayed to steer each line array in a chosen direction. Each array is comprised of correlated monopoles, with the time delay between sources as stated, but the two arrays are mutually incoherent. As shown in Fig. 12(a), the amplitude of the noise is spatially weighted according to a Rayleigh distribution, centered at a chosen location downstream. Each source distribution is given a spectral shape according to two Butterworth bandpass filters, as displayed in Fig. 12(b). This source representation is intended to simulate some spectral overlap between the two sources, so that from 125 to 315 Hz the dominant radiation transitions from one source to the other, with contributions from both sources at intermediate frequencies. The lower and higher-frequency sources are centered at 10.5 and 5 m downstream, and steered with directionalities of 130 and 115 degrees, respectively. These parameters are chosen to correspond to the approximate source locations indicated by intensity ray-tracing and intensity vector directions from the 3 dB-down regions shown previously in Fig. 6.
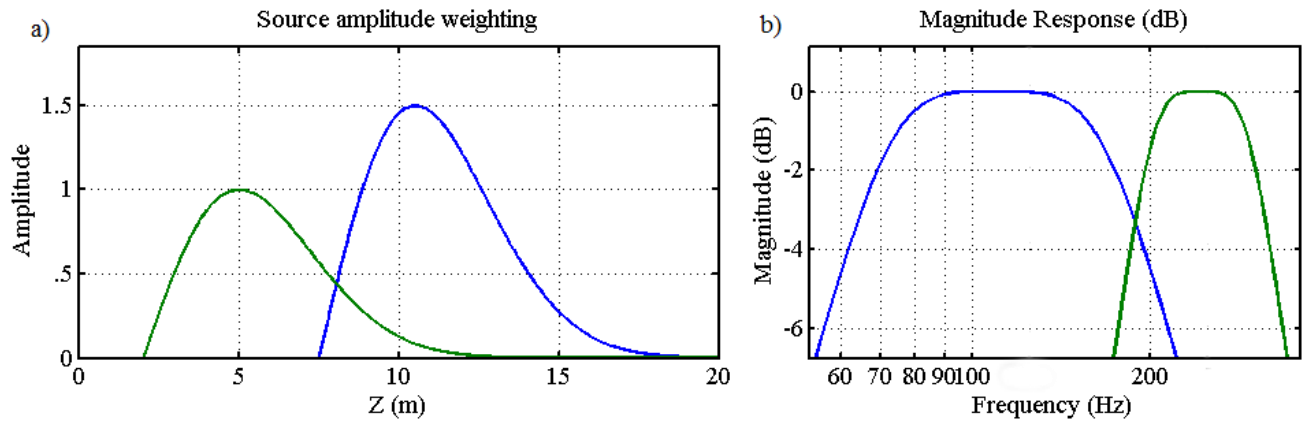
FIGURE 12. (a) Location-dependent amplitude weightings of the monopole arrays, and (b) spectral response of filters applied to the noise from both correlated arrays. Coloring for each array is consistent between (a) and (b). The locations were chosen based on intensity measurement results, with centers at Z = 5 m and Z = 10.5 m downstream.

The measured and simulated intensities for two frequencies of interest are shown in Fig. 13. For each measurement location, the simulated intensity is found by calculating the complex pressures and cross spectra at four positions corresponding to a simulated intensity probe. With the simple, overlapping equivalent source model, the simulated intensity results exhibit the same basic trends as the measured intensity. At 160 Hz, mixing between the two independent sources is apparent, with one directionality dominating at 20-25 m downstream, and the other at 6-12 m downstream. At 200 Hz, radiation from the upstream source dominates. The contribution from the second source at 200 Hz (at 20-25 m) is not well represented in the simulation, however, likely due to the assumed spatial extent and spectrum of the sources. Though this simulation represents an initial, nonoptimized attempt at an equivalent source model, it shows the feasibility of two correlated arrays which are mutually incoherent in explaining the intensity measurement trends.
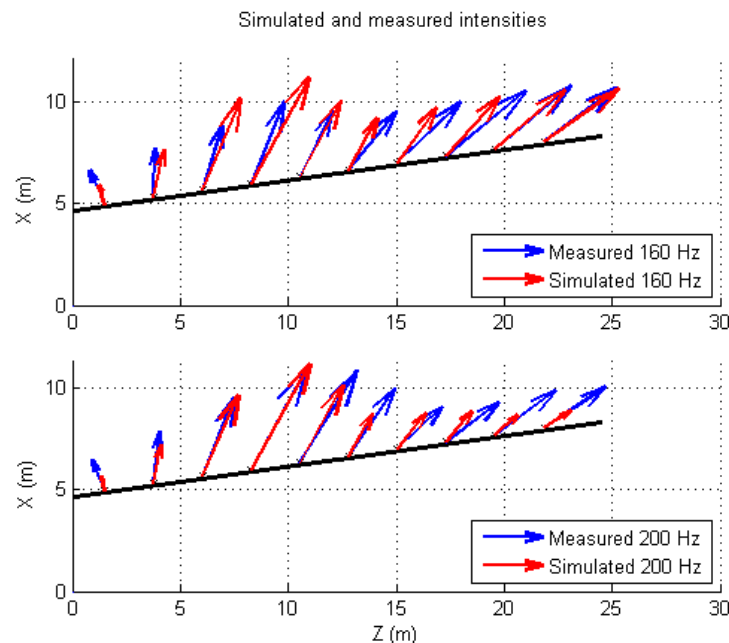

FIGURE 13. Intensity simulated at the first measurement plane due to the two correlated line arrays, for 160 Hz (top) and 200 Hz (bottom). The simulation is overlaid onto measurements at 160 Hz and 200 Hz for military engine condition (blue arrows).

CONCLUSION

This preliminary intensity-based analysis of intensity probe measurements near an F-22 provide a vector description of the noise field. In addition, single-frequency intensity vectors in the maximum region can be traced back to the source to provide an approximate maximum source region. The frequency variation in the estimated source regions follow trends expected for high-power jets. The intensity results around 200 Hz have two maxima, which supports previous observations that there are perhaps two mutually incoherent sources producing a double spectral peak in the maximum radiation direction for high-performance military jet engine noise, which are not seen in laboratory-scale jets.

To further investigate this feature, an equivalent source simulation has been used to model the intensity resulting from two discrete broadband sources, which are spatially overlapped but mutually incoherent. The intensity simulations tend to agree well with intensity measurements near the F-22. In general, these results confirm the plausibility of two self-correlated, mutually uncorrelated sources with distinct spectral characteristics dominating the full-scale jet radiation in the peak-frequency region. The simulation shows the advantage of an equivalent source model in investigating how the peak-frequency region might be represented by two directional line arrays of monopoles, rather than one. Further work may extend this modeling technique in the effort to improve current theories of jet noise, and account for the anomalous discrete nature of the military fighter jet spectrum in the maximum radiation region.

ACKNOWLEDGMENTS

REFERENCES

1. S. R. Ventakesh, D. R. Poak, and S. Narayana, "Beamforming algorithm for distributed source localization and its application to jet noise," AIAA J. **41**, 1238–1246 (2003).

2. M. Lee and J. S. Bolton, "Source characterization of a subsonic jet by using near-field acoustical holography," J. Acoust. Soc. Am. **121**, 967–977 (2007).

3. A. T. Wall, K. L. Gee, M. D. Gardner, T. B. Neilsen, and M. M. James, "Near-field acoustical holography applied to high-performance jet aircraft noise," Proc. Mtgs. Acoust. **9**, 040009 (2011).

4. A. T. Wall, K. L. Gee, T. B. Neilsen, D. W. Krueger, M. M. James, S. D. Sommerfeldt, and J. D. Blotter, "Full-scale jet noise characterization using scan-based acoustical holography," AIAA Paper 2012–2081, June (2012).

5. S. M. Jaeger and C. S. Allen, "Two-dimensional sound intensity analysis of jet noise," AIAA Paper No. 93-4342 (1993).

6. K. L. Gee, J. H. Giraud, J. D. Blotter, and S. D. Sommerfeldt, "Near-field vector intensity measurements of a small solid rocket motor," J. Acoust. Soc. Am. **128**, EL69–EL74 (2010).

7. K. L. Gee, J. H. Giraud, J. D. Blotter, and S. D. Sommerfeldt, "Energy-based acoustical measurements of rocket noise," AIAA Paper 2009-3165, May (2009).

8. M. M. James and K. L. Gee, "Advanced acoustic measurement system for rocket noise source characterization," Proc. Internoise 2012, paper in12_1127 (2012).

9. A. T. Wall, K. L. Gee, M. M. James, K. A. Bradley, S. A. McInerny, and T. B. Neilsen, "Near-field noise measurements of a high-power jet aircraft," Noise Control Eng. J. **60**, 421–434 (2012).

10. M. M. James and K. L. Gee, "Aircraft jet plume source noise measurement system," Sound Vib. **44**, 14–17 (2010).

11. T. B. Neilsen, K. L. Gee, A. T. Wall, and M. M. James, "Similarity spectra analysis of high-performance jet aircraft noise," J. Acoust. Soc. Am. **133**, 2116–2125 (2013).

12. T. B. Neilsen, K. L. Gee, A. T. Wall, M. M. James, and A. A. Atchley, "Comparison of supersonic full-scale and laboratory-scale jet data and the similarity spectra for turbulent mixing noise," Proc. Mtgs. Acoust. **19**, 040071 (2013).

13. A. T. Wall, K. L. Gee, T. B. Neilsen, and M. M. James. "Acoustical holography imaging of full-scale jet noise fields." INTER-NOISE and NOISE-CON Congress and Conference Proceedings. **246**, 1 (2013).

14. A. T. Wall, K. L. Gee, T. B. Neilsen, and M. M. James, "Partial field decomposition of jet noise sources using optimally located virtual reference microphones," Proc. Mtgs. Acoust. **18**, 045001 (2012).

15. J. Morgan, T. B. Neilsen, K. L. Gee, A. T. Wall, and M. M. James, "Simple-source model of high-power jet aircraft noise," Noise Control Eng. J. **60**, 435–449 (2012).

16. F. Jacobsen, "Sound intensity and its measurement and applications," Acoustic Technology, Technical University of Denmark (2006).

17. J.-C. Pascal and J.-F. Li, "A systematic method to obtain 3D finite-difference formulations for acoustic intensity and other energy quantities," J. Sound Vib. **310**, 1093–1111 (2008).

18. S.S. Lee and J. Bridges, "Phased-array measurements of single flow hot jets", AIAA paper 2005-2842, (2005).

19. SBIR DATA RIGHTS - (DFARS 252.227-7018 (JUNE 1995)); Contract Number: FA8650-08-C-6843; Contractor Name and Address: Blue Ridge Research and Consulting, LLC, 29 N Market St, Suite 700, Asheville, NC Expiration of SBIR Data Rights Period: March 17, 2016 (Subject to SBA SBIR Directive of September 24, 2002) The Government's rights to use, modify, reproduce, release, perform, display, or disclose technical data or computer software marked with this legend are restricted during the period shown as provided in paragraph (b)(4) of the Rights in Noncommercial Technical Data and Computer Software—Small Business Innovation Research (SBIR) Program clause contained in the above identified contract. No restrictions apply after the expiration date shown above. Any reproduction of technical data, computer software, or portions thereof marked with this legend must also reproduce the markings. Distribution A – Approved for Public Release; Distribution is Unlimited 88ABW-2013-4808.